Investigation of the structure, phase composition, and electrochemical characteristics of hydrogen-sorbing intermetallics of the La–Mg–Ni system obtained by the sintering method

Artem V. Krynytskyi[a], Larysa H. Shcherbakova, Kateryna O. Hraivoronska, Anatolii V. Sameliuk, Yurii M. Solonin

[a] *Frantsevich Institute for Problems of Materials Science of NASU*

3, Krzhizhanovsky str., Kyiv, 03142, Ukraine

contacting e-mail: ar.krynytskyi@gmail.com

Keywords: *sintering*, *phase composition*, *discharge capacity, kinetics, cyclic stability*

The crystal structure, phase composition, and electrochemical properties of the materials obtained by sintering of ($LaNi_3$+Mg+Ni) powder mixture in the temperature range 640–1020°C have been investigated. Experimental results show that, at temperatures of ≤850°C, the sintered multiphase material, whose major phases are phases with $PuNi_3$-type structure ($LaMg_2Ni_9$ and $LaNi_3$) and $CaCu_5$-type structure ($LaNi_5$), is formed. With increase in temperature, the number of phases in the sintered material decreases to a single major phase $LaNi_5$, and the content of the $LaMg_2Ni_9$ phase practically does not change. It has been established that increase in sintering temperature deteriorates the activation of the electrode materials and slows down the hydrogen absorption process. At the same time, the maximum discharge capacity and cyclic stability of electrodes increase.

Introduction

The nature of the electrode material is one of the main factors that influence the operation of secondary metal-hydride–nickel (Ni–MH) batteries. For the last 20 years, AB_5-type $LaNi_5$-extensively used as materials of cathodes for this type of batteries. But their small discharge capacity (up to 320 mA·h/g) will limit their application in batteries with a high energy density in the future. For the last 10–15 years, hydrogen-sorbing La–Mg–Ni-based alloys of AB_3 type attracted attention of researchers because the electrochemical capacity of some of them was 20–25 % higher (to 400 mA·h/g) than that of commercial AB_5-type alloys [1, 2]. The chemical and phase composition, the structure, materials substantially influence electrochemical characteristics of these alloys and depend to a great extent on the method of their preparation and subsequent treatment [2–4]. Difficulties in introduction of magnesium during melting impelled researchers to develop new techniques and conditions for multistage

production of La–Mg–Ni-based intermetallics of AB_3 type. Kadir and colleagues [5] have synthesized successfully a number of new RMg_2Ni_9 ternary alloys (where R is a rare earth metal) by sintering of mixtures of $MgNi_2$ with RNi_5-type intermetallics or by direct sintering of elements taken in the atomic ratio R:Mg:Ni = 1:2:9. Using similar sintering process, Chen, Liao and colleagues [6, 7] obtained several types of R–Mg–Ni-based alloys with $PuNi_3$-type structure.

The aim of the present work was to investigate the possibility of obtaining of hydrogen-sorbing La–Mg–Ni-based alloys of AB_3 type by sintering of ($LaNi_3$+Mg+Ni) powder mixture as well as to study their structure, phase composition and electrochemical characteristics depending on the temperature conditions of sintering.

Experimental part

Material and methods

To obtain the (La–Mg–Ni)-based compounds the $LaNi_3$ alloy, MPF-4 magnesium and PNE-1 nickel powders were used as initial materials. The amount of magnesium in the mixture was taken with an excess of 0.1% of its calculated amount. The indicated materials were mixed manually for about 2 h with the addition of a small amount of alcohol to prevent exfoliation. Then the mixture was compacted in pellets of 1.0 cm in diameter with a weight of about 1 g.

The phase composition and structure of specimens of the alloys were investigated by the X-ray diffraction method using DRON 3M diffractometer with the Bragg-Brentano focusing scheme. X-ray diffraction patterns were recorded in Cu K_α monochromatic radiation in the 2θ range of 20–80° with a scanning step of 0.05°. X-ray diffraction patterns were processed using the SciDAVis 1.D009 program. Micrographs of the surface of the electrodes and distribution of magnesium in electrodes were obtained by the X-ray mapping method with the use of the Superprobe 733 X-ray microanalyzer (JEOL, Japan).

Electrochemical measurements for electrodes, made of alloys powders, were performed in a standard electrochemical cell in a 30% KOH electrolyte with a platinum counter electrode and mercury-oxide (Hg/HgO) reference electrode. PGSTAT4-16 computer-aided potentiostat-galvanostat and Charge4Chan galvanostat were used in the work. Electrodes were made in the form of pellets of 0.8 cm in diameter from mixture of alloy powder (0.05 g) and copper (0.15 g), which was pressed onto a nickel grid. To activate the surface and to reduce partially oxidized binder (copper) powder, the electrodes were subjected to contact activation in pair with a Zn anode for 10 min in a 30% KOH solution. Kinetic characteristics of reversible absorption of hydrogen by the obtained electrodes were investigated with the help of cyclic voltammetry (CVA) within the potential

range (–1.2 V) ≤ E ≤ (–0.6 V), the scan rate of potential being increased gradually from 1 to 50 mV/s. The dependence of the maximum anodic current (i_{an}) of oxidation of hydrogen, absorbed by the electrode, versus the potential scan rate (i_{an}–$V^{-1/2}$) was used to determine the stages limiting the discharge process.

The electrodes were charged and discharged by currents of 80 mA/g, and the discharge cut-off potential was set to –0.6 V. All potentials were referred to the Hg/HgO reference electrode.

Synthesis

Sintering of specimens of the alloys was carried out in a quartz reactor, which was triply filled by purified argon from an argon cylinder after preliminary evacuation to remove air. The purification of argon from oxygen traces was performed by passing it through a quartz tube filled by zirconium chips heated to 800°C. Argon was also purified from water traces by passing it through a column filled by P_2O_5 powder. Pressure in the system was controlled with the help of two reducers.

To reduce magnesium loss during sintering, a two-stage scheme of heating of the initial powder mixture was used. During the first stage of sintering, heating of specimens was carried out at a temperature lower than the melting point of magnesium (640°C) for 2 h. Reactive sintering of the alloys was performed during the second stage at temperatures of 850°C, 950°C and 1020 °C for 4 h.

Results and discussion

The introduction of magnesium during the first sintering stage led to a substantial change of the composition of the initial mixture (**Figure** 1, curve 2). According to the XRD data, the material obtained by sintering at 640°C contained 4 phases (**Table** 1). Its major phases were those of $PuNi_3$-type and $CaCu_5$-type structures, and the Mg_2Ni phase was present in amounts evaluated as traces.

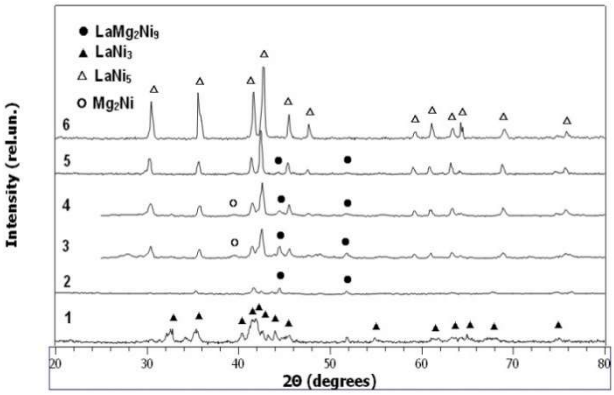

Figure 1. X-ray diffraction patterns obtained on specimens of $LaNi_3$ (1), $LaNi_5$ alloys (6) and specimens sintered at different temperatures (°C): 640 (2); 850 (3); 950 (4); 1020 (5).

Table 1. Characteristics of phases in initial and sintered at 640°C specimens

Materials	Type of the structure	Space group	Volume of lattice
$LaNi_3$*	$PuNi_3$	$R\bar{3}m$	557.40
$LaNi_5$*	$CaCu_5$	P6\mmm	86.68
Material sintered at 640°C			
$LaNi_3$	$PuNi_3$	$R\bar{3}m$	556.01
$LaNi_5$	$CaCu_5$	P6\mmm	86.39
$LaMg_2Ni_9$	$PuNi_3$	$R\bar{3}m$	500.18
Mg_2Ni	B_2Al	$P6_222$	310.55

- *- PCPDFWIN (Version 2.0)

After the first stage of sintering (640°C), a homogeneous distribution of magnesium-containing phases in the volume of the material is observed (**Figure 2**).

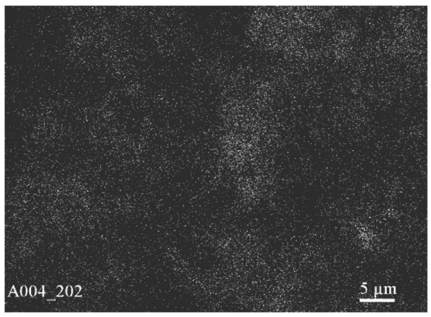

Figure 2. Distribution of magnesium in the electrode sintered at 640°C (see **Figure** 5a).

From the dependences of the maximum anodic current versus the potential scan rate (i_{an}–$V^{-1/2}$) obtained for electrodes made of $LaNi_3$ and $LaNi_5$ alloys and for electrode made of multiphase material, sintered at 640°C, it follows that the discharge process is controlled both by the diffusion of hydrogen in the volume of the electrode and by the stage of its discharge on the electrode surface (mixed diffusion–kinetic control) (**Figure** 3, curves 1, 2 and 6).

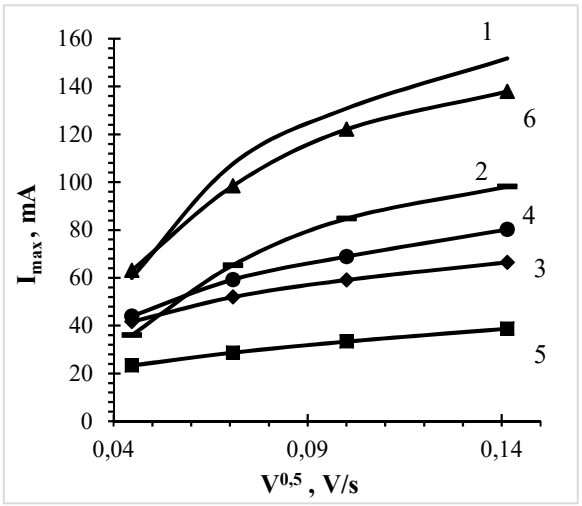

Figure 3. Dependence of the maximum rate of anodic hydrogen oxidation versus polarization rate for the electrodes made: of $LaNi_3$ (1) and $LaNi_5$ (6) alloys, and of sintered materials (2–5). Sintering temperatures of powders (°C): 640 (2); 850 (3); 950 (4); 1020 (5).

The discharge capacity of the electrodes made of the multiphase material obtained at 640°C, despite the high content of the $LaNi_5$ phase in it, is close to that of the electrode made of the $LaNi_3$ alloy (about 130 mA·h/g). This is half the capacity of the electrode made of the cast $LaNi_5$ alloy (about 275 mA·h/g) (**Figure** 4, curves 1, 2 and 6).

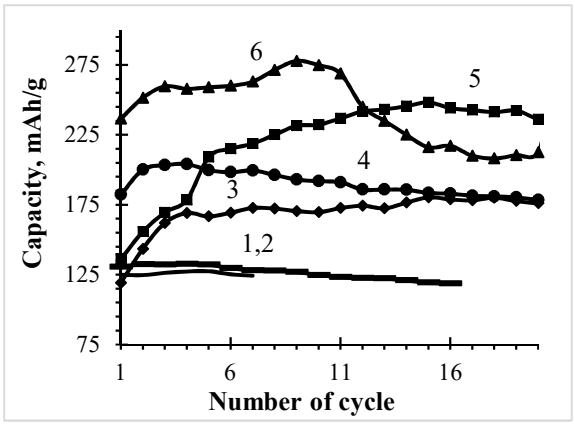

Figure 4. Cyclic stability of electrodes made: of $LaNi_3$ (1) and $LaNi_5$ (6) alloys, and of sintered materials (2-5). Sintering temperatures of powders (°C): 640 (2); 850 (3); 950 (4); 1020 (5).

The results of the investigation of the structure and phase composition of the materials after sintering of specimens during the second stage indicate their dependence on the sintering temperature: with increase in the temperature, the number of phases in the sintered material decreases to a single major phase, namely, $LaNi_5$ (**Figure** 1, curves 3–5).

The microstructure of the sintered materials changes substantially with change in the temperature regime of their preparation: sintering at temperatures of 950°C and above leads to the coarsening of alloy grains and to formation of pores in them (**Figure** 5).

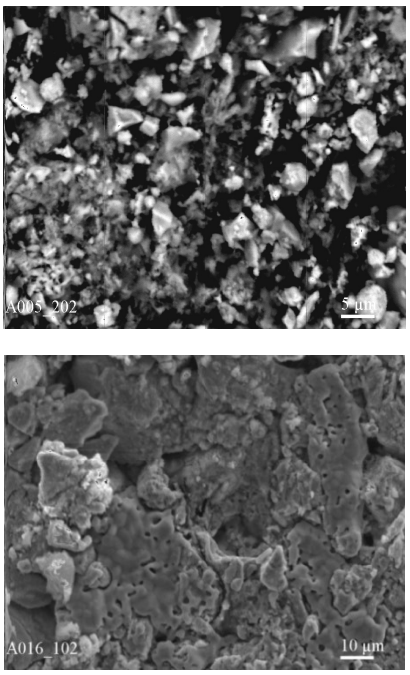

Figure 5. Micrographs of surface of specimens of the alloys (SEI, x2000) after sintering at different temperatures (°C): (a) 640; (b) 1020.

Dependences of the reversible hydrogen absorption, maximum discharge capacity and its variation in cycling on the sintering temperatures are established. Despite the fact that the $LaNi_5$ phase is the major phase of the sintered alloys, the overvoltage of the cathodic process and the rate of its realization are much smaller than those for the electrode made of the cast $LaNi_5$ alloy, and these differences increase with rise in the temperature. In the region of discharge potentials, the hydrogen desorption process on the sintered materials is limited by its diffusion in the volume of the electrode (the dependence i_{an}–$V^{-1/2}$ is linear) (**Figure** 3, curve 3–5) in contrast to the electrodes made of the $LaNi_5$ alloy (mixed control), (**Figure** 3, curve 6). The annealing (800°C, 5 hours) of the sintered materials deteriorates the kinetics of both these processes.

The activation of the alloys deteriorates with increase in the sintering temperature during its preparation: the number of activation charge/discharge cycles increases from 3–5 for electrodes obtained at a temperature of 850°C to 10–14 cycles for electrodes obtained at temperatures above 950°C. It is established that the maximum discharge capacity of the electrodes ($C_{max.}$) increases substantially with increase in the temperature of preparation of the material: electrodes made of the materials sintered at 1020°C exhibit the highest discharge capacity equal to 248 mA·h/g (**Figure** 4, **Table** 2).

Table 2. Maximum discharge capacity and cyclic stability of investigated alloys

Materials	$C_{max.}$, мА×h/g	$C_{20c.}$, мА×h/g	$C_{max.}$/ $C_{20c.}$, %
$LaNi_5$	278.0	212.0	76.4
$LaNi_3$	127. 5	110.0	87.1
Sintering at 650°C, 2h	132.6	120.0	90.5
850°C, 4h	170.0	109.0	88.5
950°C, 4h	180.0	176.0	97.7
1020°C, 4h	248.0	245.0	98.7

The investigation of the behavior of the electrodes made of the sintered materials during reversible hydrogen absorption shows that the capacity loss in the first 20 charge/discharge cycles ($C_{20c.}$) is smaller for the electrodes made

of the sintered materials than for the electrode made of the cast $LaNi_5$ alloy (**Table** 2).

It is established that the $LaNi_5$ alloy formed during sintering differs from the cast analog by increased lattice parameter ***a*** and increased (by 0.7–1.5%) volume of the unit cell. This can be connected with the partial oxidation of alloy particles during sintering, as a result of which the activation and kinetic characteristics of the sintered $LaNi_5$-based alloys deteriorate.

Conclusions

The results of the investigation of the structure and phase composition of the specimens of alloys obtained by sintering of the ($LaNi_3$+Mg+Ni) powder mixture in the temperature range 640–1020 °C show that materials obtained by sintering at 850°C contain several phases such as $LaNi_3$, $LaNi_5$, $LaMg_2Ni_9$ and an impurity of the $MgNi_2$ phase. With increase in the sintering temperature, the content of phases with $PuNi_3$-type structure (**(**$LaNi_3$ and $LaMg_2Ni_9$ phases) decreases, whereas the content of the $LaNi_5$ phase increases. It has been established that with increase in the sintering temperature, the value of the maximum discharge capacity and cyclic stability of electrodes made of the sintered alloys increase. The alloy obtained by sintering at temperature of 1020°C exhibits the highest value of the maximum discharge capacity (248 mA·h/g). It has been shown that it is unreasonable to perform additional annealing (at 850°C for 5 h) of sintered specimens.

References

[1] Li Y., Han S.V., Li J.H., Zhu X.L., Hu L. Study of kinetics and electrochemical properties of $Ml_{0,79}Mg_{0,30}(Ni_{3.95}Co_{0,75}Mn_{0,15}Al_{0,15})_x$ (x=0,6, 0.64,0.68 0.70 ,0.78) alloys. Mater.Chem.Phys. 2008; 108 (1):92-96

[2] Liao B., Lei Y.O., Chen L.X. et.al Effect of La/Mg ratio on the structure and electrochemical properties of $LaxMg_{3-x}Ni_9$ (x=1.6-2.2) hydrogen storage electrode alloys for nickel-metal hydride batteries. J.Power Sources 2004; 129 (1):358-367.

[3] Dong Zh., Wu Ya. Ma L., Wang L. et al. Electrochemical hydrogen storage properties of non stoichiometric $La_{0,7}Mg_{0,3-x}Ca_xNi_{2,8}Co_{0,5}$ (x=0-0.1) electrode alloys. J.Alloys Comp. 2011; 509(17):5280-5284.

[4] Nwakwuo Ch. C., Holm Th., Denys R. V., Hu W., Maehlen Ja. P., Solberg Ja. K., Yartys A. V. Effect of magnesium content and quenching rate on the phase structure and composition of rapidly solidified La_2MgNi_9 metal hydride battery electrode alloys. J.Alloys Comp. 2013; 555:201-208.

[5] Kadir K., Sakai T., Uehara I. Structural investigation and hydrogen storage capacity of $LaMg_2Ni_9$ and $(La_{0.65}Ca_{0.35})(Mg_{1.32}Ca_{0.68})Ni_9$ of the AB_2C_9 type structure. J.Alloys Comp. 2000; 302 (1-2):112-117.

[6] Liao B., Lei Y.Q., Lu G.L., Chen L.X., Pan H.G., Wang Q.D. The electrochemical properties of $La_xMg_{3-x}Ni_9$ (x=1.0–2.0) hydrogen storage alloys J. Alloys Comp. 2003; 356–357:746–749.

[7] Liao B., Lei Y.Q, Chen L.X, Lu G.L, Pan H.G, Wang Q.D A study on the structure and electrochemical properties of $La_2Mg(Ni_{0.95}M_{0.05})_9$ (M = Co, Mn, Fe, Al, Cu, Sn) hydrogen storage electrode alloys. J.Alloys Comp. 2004; 376 (1-2):186-195.